Available online at www.sciencedirect.com
ScienceDirect
Atmospheric Environment 42 (2008) 4198–4211
ATMOSPHERIC ENVIRONMENT
www.elsevier.com/locate/atmosenv

Reductions in ozone concentrations due to controls on variability in industrial flare emissions in Houston, Texas

Junsang Nam[a], Mort Webster[b,*], Yosuke Kimura[c], Harvey Jeffries[d], William Vizuete[d], David T. Allen[c]

[a]*School of Earth and Atmospheric Sciences, Georgia Institute of Technology, 311 Ferst Drive, Atlanta, GA 30332, USA*
[b]*Department of Earth, Atmosphere, and Planetary Sciences, Massachusetts Institute of Technology, E40-408, 77 Massachusetts Avenue, Cambridge, MA 02139, USA*
[c]*Center for Energy and Environmental Resources, University of Texas, 10100 Burnet Road, M/S R7100, Austin, TX 78758, USA*
[d]*Department of Environmental Sciences and Engineering, School of Public Health, University of North Carolina, Chapel Hill, NC 27599, USA*

Received 17 August 2007; received in revised form 11 January 2008; accepted 11 January 2008

Abstract

High concentrations of ozone in the Houston/Galveston area are associated with industrial plumes of highly reactive hydrocarbons mixed with NO_x. The emissions leading to these plumes can have significant temporal variability, and photochemical modeling indicates that the emissions variability can lead to increases and decreases of 10–50 ppb, or more, in ozone concentrations. Therefore, in regions with extensive industrial emissions, accounting for emission variability can be important in accurately predicting peak ozone concentrations, and in assessing the effectiveness of emission-control strategies. This work compares the changes in ozone concentrations associated with two strategies for reducing flare emissions in Houston, Texas. One strategy eliminates the highest emission flow rates, that occur relatively infrequently, and a second strategy reduces emissions that occur at a nearly constant level. When emission variability is accounted for in air quality modeling, these control scenarios are both predicted to be much more effective in reducing the expected value of daily maximum ozone concentrations than if similar reductions in the mass of emissions are made and constant emissions are assumed. The change in the expected value of daily maximum ozone concentration per ton of emissions reduced, when emissions variability is accounted for, is 5–10 times the change predicted when constant (deterministic) inventories are used. Strategies that eliminate the infrequent largest emissions are more effective at reducing the highest localized ozone concentrations than changes in nearly constant emissions.

Keywords: Photochemical grid model; Highly reactive volatile organic compounds (HRVOC); Ozone; Uncertainty analysis

1. Introduction

The Houston/Galveston (HG), area, like many large urban areas in the United States, exceeds the National Ambient Air Quality Standards (NAAQS) for ground-level ozone with concentrations

*Corresponding author. Tel.: +1 617 253 3901; fax: +1 617 253 9845.
E-mail address: mort@mit.edu (M. Webster).

1352-2310/$ - see front matter © 2008 Elsevier Ltd. All rights reserved.
doi:10.1016/j.atmosenv.2008.01.035

averaged over 1 and 8 h. Unlike other urban areas in the United States, however, changes in observed ozone concentrations in the HG area are rapid (up to 200 ppb h^{-1}) and efficient (up to 10–20 moles ozone formed per mole of NO_x consumed). These unique characteristics of ozone formation in the HG area are associated with plumes of reactive hydrocarbons, emanating from the industrial Houston Ship Channel area (Kleinman et al., 2003; Ryerson et al., 2003). Therefore, understanding industrial emissions, particularly of reactive hydrocarbons, is critical in the development of control measures for mitigation of high ozone concentrations in the area.

Industrial emissions of hydrocarbons, from sources other than electricity generating units (non-EGU), have traditionally been assumed to be continuous at constant levels for air quality regulation and photochemical modeling purposes. However, ambient observations and industrial process data from the HG area have shown that non-EGU industrial emissions of hydrocarbons have significant temporal variability (Murphy and Allen, 2005; Webster, et al., 2007). Variability in non-EGU industrial emissions of hydrocarbons in the HG area can be ascribed to both the occurrence of episodic emission events and variable continuous emissions. The episodic emission events are non-routine discrete emission events, of more than permitted amounts, with reporting required under Texas law. Episodic events occur relatively infrequently; an emission event of more than 1000 kg occurs, on average, a few times a week somewhere among the hundreds of facilities and the thousands of non-EGU industrial emission points in the Houston area (Murphy and Allen, 2005). So, at any single facility or process unit, an emission event is a rare occurrence, but collectively, over the entire region, large emission events (>1000 kg) occur weekly. Nam et al. (2006) performed photochemical modeling of hundreds of emission events, and concluded that only a small percentage of the events lead to large increases in ozone concentrations. Approximately 1.5% of emission events produced more than 10 ppb of additional ozone, and 0.5% of emission events produced more than 70 ppb of additional ozone, compared to base case photochemical modeling simulations with no emission events. Emission events that exceed permitted levels are not considered in this study.

Variable continuous emissions are not as significant in magnitude as emission events, when the events occur, but variability in continuous emissions occurs at all times, at many facilities and process units, and therefore also have the potential in aggregate to increase the magnitude of ozone concentration in the HG area. Webster et al. (2007) described the variability in routine hydrocarbon emissions from non-EGU industrial sources in terms of three emission modes: nearly constant emissions, routinely variable emissions and allowable (within permitted levels) episodic emissions. Each mode was described for multiple sources, such as flares, cooling towers, and process vents and area-wide emissions from these industrial sources were modeled for the HG area. Air quality simulations indicated that variability in industrial emissions had the potential to cause increases and decreases of 10–50 ppb, or more, in hourly ozone concentration, as compared to simulations with the same total emissions, but industrial non-EGU emissions that are assumed to be constant. The largest of these differences were predicted to be confined to small areas (10–20 km^2), but the emission variability also had the potential to increase region wide maxima in hourly ozone concentrations by up to 12 ppb.

These results indicate that variability in industrial non-EGU emissions may be just as important to control as discrete emission events and the average magnitude of the emissions. In this study, the effect of controls that target different modes of emissions considered by Webster et al. (2007), will be compared. In particular, the relative impact of controlling infrequent high emissions as opposed to reducing routine low emissions rates will be assessed. Emissions from flares will be used here as a case study. Flares are chosen as the focus because they constitute a significant fraction of industrial emissions in the HG area, and their variability was well characterized by Webster et al. (2007). In addition, Flare Minimization Plans (FMPs) have been prepared by petroleum refineries in the San Francisco Bay Region, as required by the Bay Area Air Quality Management District (BAAQMD, 2005, 2006). These minimization plans provide insight into the types of controls that can be used to reduce different modes of flare emission variability. It will be shown that, to reduce the highest localized ozone concentrations, a strategy that reduces infrequent large magnitude emissions is more effective than controlling emissions from normal operating conditions.

2. Methods

2.1. The stochastic emission inventory for the HG area

Webster et al. (2007) indicated that continuous industrial emissions of volatile organic compounds (VOC) have significant temporal variability and that the variability is composed of multiple components, including nearly constant, routinely variable, and allowable episodic emissions. As shown in Fig. 1, emission events above permitted levels also occur, but the analysis presented in this work will consider only emissions that are within permitted values. Nam et al. (2006) report on the impacts of discrete emission events above permitted levels. Webster et al. (2007) simulated industrial emissions using probability distribution functions (PDFs) for three emission modes (nearly constant, routinely variable and allowable episodic). The choice of this approach was based on data from flares and cooling towers in the HG area.

The goal of this work is to compare the relative impacts on hourly ozone concentrations of controlling the allowable episodic emissions (least frequent but largest magnitude of variability) with controlling the nearly constant emissions (most frequent but smallest magnitude of variability) from flares. To model these control strategies, it was necessary to modify the stochastic emission inventory generator. The original version of the stochastic emission inventory generator (Webster et al., 2007) randomly selects the next emission mode (nearly constant, routinely variable, or allowable episodic modes), the time duration in that mode, and hourly emission rates while in that mode. The emission modes, durations in each mode, and emission rates are sampled from PDFs based on data from observed industrial flares. In this analysis, we introduce a modified version of the stochastic inventory generator that models the emissions variability as a Markov process. A Markov process is a system in which the conditional probability distribution over future states is dependent on the current state of the process. A Markov process is described by a transition matrix, in which the row index (i) represents the current mode and the column index (j) represents the next mode; the entries in the matrix represents the probability of transition from the current mode (i) to the next mode (j), P_{ij}. The transition matrix probabilities for 10 models of flares based on observations are given in Table 1. For example, for Flare 1, probabilities of a transition from mode 1 to modes 1, 2, and 3, in the

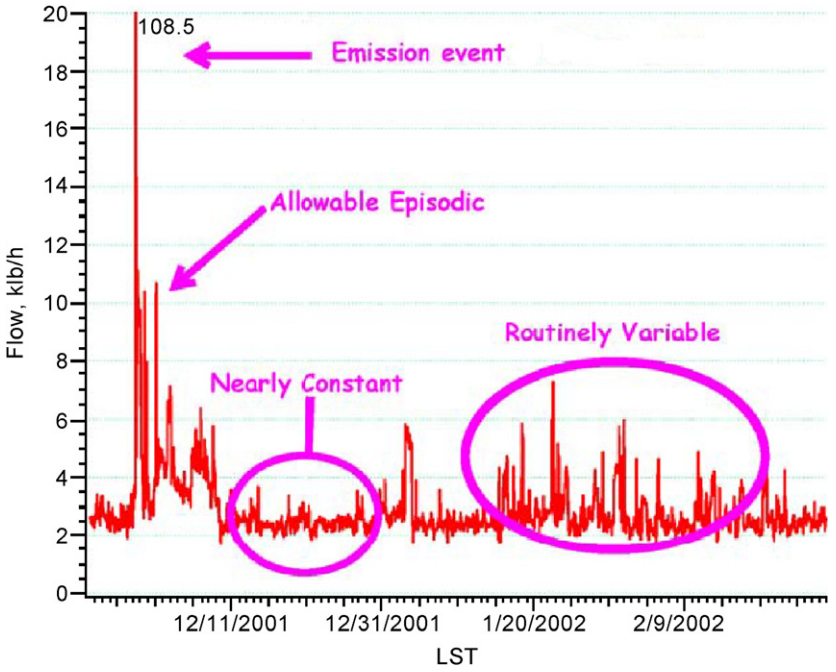

Fig. 1. Components of mass flow rates to a flare at an industrial facility in the HG area: nearly constant, routinely variable, allowable episodic, and emission event in order of magnitude (Webster et al., 2007).

Table 1
Arameters for observations from emission sources

Flare name	Mode[b]	Normal or lognormal	Mean or mean (LN value)[a]	Standard deviation	Normalized proportion	Transition matrix			Shift	Expected values
Flare1	1	N	2.43	0.26	0.603	0.883	0.115	0.001	0.0	2.4
	2	LN	−0.80	1.05	0.389	0.179	0.813	0.008	2.8	3.5
	3	LN	1.26	0.50	0.008	0.085	0.380	0.535	5.1	9.1
Flare2	1	N	1.97	0.64	0.544	0.798	0.196	0.005	0.0	2.0
	2	LN	0.54	0.97	0.426	0.252	0.729	0.020	2.8	5.6
	3	LN	−0.75	1.65	0.029	0.048	0.333	0.619	11.0	12.8
Flare5	1	LN	6.80	0.31	0.763	0.951	0.022	0.027	42.6	983.2
	2	N	2017.00	114.80	0.061	0.290	0.557	0.154	0.0	2017.3
	3	LN	5.98	0.72	0.176	0.113	0.058	0.829	2153.2	2665.6
FCCU	1	N	21.10	3.01	0.906	0.997	0.002	0.001	0.0	21.1
	2	N	33.67	2.14	0.072	0.032	0.958	0.010	0.0	33.7
	3	LN	0.95	0.69	0.022	0.003	0.058	0.939	37.6	40.8
General service 1	1	N	21.40	1.51	0.946	0.990	0.009	0.001	0.0	21.4
	2	LN	−0.57	1.44	0.040	0.218	0.762	0.020	24.0	25.6
	3	LN	0.40	1.41	0.014	0.046	0.068	0.886	28.9	32.9
General service 2	1	N	17.08	0.94	0.670	0.970	0.027	0.003	0.0	17.1
	2	N	19.18	0.16	0.250	0.072	0.869	0.059	0.0	19.2
	3	LN	−1.61	1.48	0.080	0.022	0.186	0.792	19.5	20.1
HC	1	N	2.41	0.62	0.974	0.989	0.011		0.0	2.4
	2	LN	−0.30	0.64	0.026	0.426	0.574		4.0	4.9
Low pressure	1	N	24.64	0.92	0.692	0.988	0.012	0.000	0.0	24.6
	2	LN	0.16	0.71	0.298	0.027	0.972	0.001	25.8	27.3
	3	LN	0.08	0.56	0.010	0.011	0.039	0.950	34.8	36.0
Merox	1	N	31.90	16.23	0.056	0.896	0.091	0.012	0.0	31.9
	2	N	500.40	89.45	0.914	0.006	0.991	0.003	0.0	500.4
	3	LN	4.89	0.24	0.030	0.019	0.082	0.899	622.5	759.5
Olefins	1	N	1.67	0.41	0.661	0.973	0.027	0.000	0.0	1.7
	2	LN	0.98	0.51	0.327	0.053	0.944	0.003	2.3	5.4
	3	LN	0.38	1.02	0.012	0.045	0.045	0.909	16.9	19.3

[a]Emissions in klb h^{-1}, except for Flare 5 and Merox flare, which are in lb h^{-1}.
[b]Emission modes are indicated as 1 = nearly constant; 2 = routinely variable; 3 = allowable episodic.

next time step, are 0.883, 0.115, and 0.001, respectively. This revised Markov process model greatly simplifies the simulation of controls on variability or extremely high emissions, because the probability of being in a particular (e.g., high) emission mode can be modified, in addition to modifying the mean emissions of each mode (Table 1).

In addition to the transition matrix, Table 1 also reports the characteristic parameters of the probability distributions for the emission modes for 10 flares on which data were collected. To develop an emission inventory for all industrial sources in the HG area, based on these data, all of the flares in the HG area are assigned one of the unit operation models. The mean of the emission variability model is scaled so that it matches the mean emissions of the specific flare under consideration. For flares, both VOC and NO_x emissions are assumed to scale with flow rate having the same pattern of variability. Details on the development of the stochastic emission inventory generator and application of the stochastic inventory to the HG area are described in Webster et al. (2007).

The revised version of the stochastic inventory generator used here also makes a second modification. The distributions for lognormal modes of the models now contain a "shift" parameter, which shifts the minimum value for which the distribution is defined from 0 to a value designated as "shift".

Table 2
Absolute error (%) in mean and selected fractiles: absolute value of (observed-simulated)/simulated)

Flare name	Mean	0.05	0.1	0.25	0.5	0.75	0.9	0.95
Flare 1	0.9	1.0	1.7	1.0	1.5	0.1	4.7	3.3
Flare 2	0.4	0.6	1.4	6.7	3.8	9.4	0.9	14.8
Flare 5	6.3	2.5	3.1	1.6	1.7	7.7	1.8	1.0
HC flare	2.8	6.3	0.1	3.5	3.4	2.3	1.2	3.0
Olefins flare	4.3	6.1	7.0	5.4	1.2	0.3	1.4	1.6
FCCU	1.7	14.2	2.9	0.9	2.6	1.1	5.6	0.7
Merox flare	2.3	84.9	2.7	0.5	2.1	1.7	4.5	7.1
Low pressure	0.1	2.1	2.5	0.6	0.6	0.8	0.4	1.4
General service #1	0.8	3.0	2.7	2.9	3.6	2.9	1.7	2.6
General service #2	1.0	1.7	1.2	1.0	1.4	0.1	0.4	0.3

Table 3
Parameters used to develop stochastic emissions with allowable episodic emissions from flares eliminated

Flare name	Mode	Normal or lognormal	Mean or mean (LN value)	Standard deviation	Normalized proportion	Transition matrix		Shift	Expected value
Flare1	1	N	2.43	0.26	0.608	0.884	0.115	0.0	2.4
	2	LN	−0.80	1.05	0.392	0.179	0.821	2.8	3.5
Flare2	1	N	1.97	0.64	0.561	0.803	0.196	0.0	2.0
	2	LN	0.54	0.97	0.439	0.252	0.749	2.8	5.6
Flare5	1	LN	6.80	0.31	0.926	0.978	0.022	42.6	983.2
	2	N	2017.00	114.80	0.074	0.290	0.711	0.0	2017.0
FCCU	1	N	21.10	3.01	0.926	0.998	0.002	0.0	21.1
	2	N	33.67	2.14	0.074	0.032	0.968	0.0	33.7
General service 1	1	N	21.40	1.51	0.959	0.991	0.009	0.0	21.4
	2	LN	−0.57	1.44	0.041	0.218	0.782	24.0	25.6
General service 2	1	N	17.08	0.94	0.728	0.973	0.027	0.0	17.1
	2	N	19.18	0.16	0.272	0.072	0.928	0.0	19.2
HC	1	N	2.41	0.62	1.000	0.000	0.000	0.0	2.4
Low pressure	1	N	24.64	0.92	0.699	0.988	0.012	0.0	24.6
	2	LN	0.16	0.71	0.301	0.027	0.973	25.8	27.2
Merox	1	N	31.90	16.23	0.058	0.908	0.091	0.0	31.9
	2	N	500.40	89.45	0.942	0.006	0.994	0.0	500.4
Olefins	1	N	1.67	0.41	0.669	0.973	0.027	0.0	1.7
	2	LN	0.98	0.51	0.331	0.053	0.947	2.3	5.4

The probability density of the lognormal distributions is defined as

$$f(x;\mu,\sigma) = \frac{e^{-(\ln(x-\text{shift})-\mu)^2/(2\sigma^2)}}{(x-\text{shift})\sigma\sqrt{2\pi}}.$$

This change enables the reduction of emissions within a specified flare flow rate regime. Table 2 compares the results of Monte Carlo simulations from each of the 10 flare models with the original flare data, showing the percentage different between the means and several fractiles of the distribution. With only a few exceptions, the differences in the cumulative distribution between observed and simulated emissions were small. As described in the results section of this paper, the revised stochastic emissions generator leads to similar distributions in predicted ozone concentrations.

2.2. Control strategies associated with variability in industrial hydrocarbon emissions

In order to understand how flare emissions can be reduced, and how those emission reductions can be modeled, it is useful to have a conceptual understanding of how a typical industrial flare system works. In many industrial operations, a flare serves multiple process units. The flare collects these multiple inputs through a collection system, or plenum, that is maintained at low pressure so that the plenum will always be at a lower pressure than the process units that it serves. Many systems that are designed to flare material with fuel value (e.g., fuel gases) are served by a compressor, so that some of the flare gases can be recycled to the facility's fuel system, which is maintained at a higher pressure than the flare system. If the flow to the flare is less than the capacity of the compressor, fuel gases that are sent to the flare system are recompressed and recycled to a process unit that uses fuel gas. If the flow is larger than can be handled by the compressor, then the fuel gas is flared. This fuel flare system is shown conceptually in Fig. 2.

With this conceptual model of flare systems in mind, two options for reducing flare emissions are (1) to add temporary storage for flared gases, so that if the flow rate to the flare goes above the capacity of the compressor, the gases can be temporarily stored, and (2) to add additional compressor capacity to a flare system.

In general, adding storage capacity for flared gases is expensive. However, temporary storage is sometimes available during start-up, shut-down, and maintenance activities (Levy et al., 2006). A flare minimization scenario that has been reported in Flare Minimization Plans by petroleum refineries is to use process vessels that are temporarily empty during start-up, shut-down, and scheduled maintenance as temporary storage for gases that would otherwise be flared during these events. This requires careful scheduling of operations during start-ups, shut-downs, and maintenance activities, but it can reduce what are often large flaring events.

Adding additional compressor capacity to a flare system is another option for increasing the amount of fuel gas that is recycled. Adding compressor capacity can also be expensive, if the compressor only recovers fuel during relatively rare emission events. However, if compressor capacity can be added to capture and recycle nearly constant flare emissions, it becomes more cost effective.

Based on these ideas, two approaches were evaluated for reducing flare emissions. The first approach is to control the large magnitude, infrequent emissions from flares (allowable episodic mode). This corresponds to eliminating large flaring events during start-up, shut-down, and maintenance activities. In modeling this approach, the allowable episodic emissions for all of the flares in the HG area were assumed to be eliminated. For this task, the stochastic inventory generator was modified to

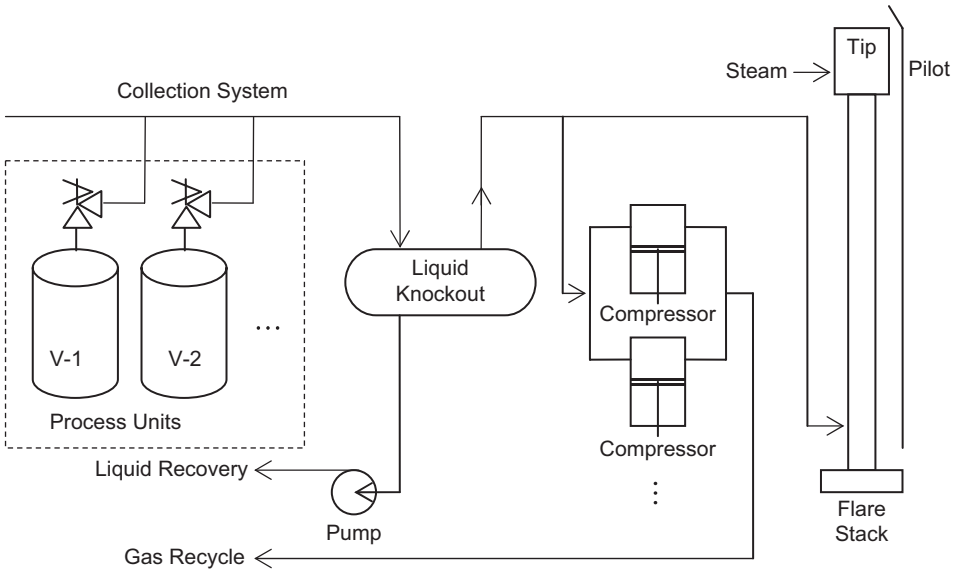

Fig. 2. Conceptual diagram for a typical refinery flare system (Shell Oil Products US, 2006).

Table 4
Parameters used to develop stochastic emissions with nearly constant emissions from flares reduced

Flare name	Mode	Normal or lognormal	Mean or mean (LN value)	Standard deviation	Normalized proportion	Transition matrix			Shift	Expected value
Flare1	1	N	1.22	0.26	0.603	0.883	0.115	0.001	0.0	1.2
	2	LN	−0.80	1.05	0.389	0.179	0.813	0.008	2.8	3.5
	3	LN	1.26	0.50	0.008	0.085	0.380	0.535	5.1	9.1
Flare2	1	N	0.99	0.64	0.544	0.798	0.196	0.005	0.0	1.0
	2	LN	0.54	0.97	0.426	0.252	0.729	0.020	2.8	5.6
	3	LN	−0.75	1.65	0.029	0.048	0.333	0.619	11.0	12.8
Flare5	1	LN	6.80	0.31	0.763	0.951	0.022	0.027	−449.0	491.6
	2	N	2017.00	114.80	0.061	0.290	0.557	0.154	0.0	2017.0
	3	LN	5.98	0.72	0.176	0.113	0.058	0.829	2153.2	2665.6
FCCU	1	N	10.60	3.01	0.906	0.997	0.002	0.001	0.0	10.6
	2	N	33.67	2.14	0.072	0.032	0.958	0.010	0.0	33.7
	3	LN	0.95	0.69	0.022	0.003	0.058	0.939	37.6	40.8
General service 1	1	N	10.70	1.51	0.946	0.990	0.009	0.001	0.0	10.7
	2	LN	−0.57	1.44	0.040	0.218	0.762	0.020	24.0	25.6
	3	LN	0.40	1.41	0.014	0.046	0.068	0.886	28.9	32.9
General service 2	1	N	8.54	0.94	0.670	0.970	0.027	0.003	0.0	8.5
	2	N	19.18	0.16	0.250	0.072	0.869	0.059	0.0	19.2
	3	LN	−1.61	1.48	0.080	0.022	0.186	0.792	19.5	20.1
HC	1	N	1.21	0.62	0.974	0.989	0.011		0.0	1.2
	2	LN	−0.30	0.64	0.026	0.426	0.574		4.0	4.9
Low pressure	1	N	12.32	0.92	0.692	0.988	0.012	0.000	0.0	12.3
	2	LN	0.16	0.71	0.298	0.027	0.972	0.001	25.8	27.3
	3	LN	0.08	0.56	0.010	0.011	0.039	0.950	34.8	36.0
Merox	1	N	16.00	16.23	0.056	0.896	0.091	0.012	0.0	16. 0
	2	N	500.40	89.45	0.914	0.006	0.991	0.003	0.0	500.4
	3	LN	4.89	0.24	0.030	0.019	0.082	0.899	622.5	759.5
Olefins	1	N	0.84	0.41	0.661	0.973	0.027	0.000	0.0	0.8
	2	LN	0.98	0.51	0.327	0.053	0.944	0.003	2.3	5.4
	3	LN	0.38	1.02	0.012	0.045	0.045	0.909	16.9	19.3

reflect this control approach, as shown in Table 3, and the stochastic inventory generated from this modified model was used to investigate the impacts on ozone formation of this emission control approach.

A second approach for reducing flare emissions is to add more compressor capacity to capture more nearly constant emissions. This approach was modeled by assuming that the nearly constant component of mass flows to all flares in the HG area was reduced by 50% in magnitude. The characteristics of the stochastic inventory generator, modified for this task, are shown in Table 4. The expected values of the models for the nearly constant emissions mode were reduced by 50%, keeping the shape of the distributions intact. The expected value for a normal distribution is its mean. Therefore, for modes with normal distributions, which include all of the nearly constant emission modes, except Flare 5[1] in Table 1, means were reduced by 50%. For example, the mean for the nearly constant emission model for Flare 1 in Table 1 were reduced from 2.43–1.22 as shown in Table 4. For lognormal distributions, however,

[1]The 10 stochastic flare models are purely based on observations. The model for Flare 5 had a significantly improved fit to its data by using a lognormal distribution for the nearly constant emission mode than did a model with a normal distribution for this mode.

expected values are a function of both mean and standard deviation (expected value $= e^{\mu+(\sigma^2/2)}$), and the shapes of lognormal distributions are determined by both mean and standard deviation (variance $= (e^{\sigma^2}-1)e^{2\mu+\sigma^2}$). Therefore, the simplest way to reduce expected value of lognormal distributions without changing the shape of the distribution is to move the distributions to the left by reducing the shift value of the model. For the nearly constant mode of Flare 5 in Table 4, the shift value was reduced so that the expected value is 50% of the original expected value shown in Table 1 (expected value $= e^{\mu+(\sigma^2/2)} + \text{shift}$); when the distribution was moved to the left by $-449\,\text{lb}\,\text{h}^{-1}$, the expected value for the distribution was reduced 50%, to $491.6\,\text{lb}\,\text{h}^{-1}$ ($E(X)_{\text{WO/Control}} = e^{6.8+(0.305^2/2)} + 42.64 = 983.2$, $E(X)_{\text{NC Control}} = e^{6.8+(0.305^2/2)} - 449 = 491.6$).

2.3. Air quality modeling

The effectiveness of the control strategies, described in the previous sub-section, was assessed using the Comprehensive Air Quality Model with extensions (CAMx) (Environ, 2004). In this work, a computationally efficient version of CAMx, referred to as a sub-domain model, was used. The overall strategy in developing the sub-domain model was to (1) identify a geographical region (sub-domain) from a full, 3-D photochemical model simulation, (2) create a computationally efficient photochemical model of the sub-domain, and (3) analyze many scenarios of variable emissions using the sub-domain model. Steps 1 and 2 in the development of the model are analogous to the methods used by Nam et al. (2006) and Webster et al. (2007) and are only summarized here. Step 3 is described in the results section.

The geographical region (sub-domain) to be modeled is the HG 1 km domain, shown as the region in red in Fig. 3. CAMx simulations using the full domain, shown in Fig. 3, were used to develop boundary and initial conditions for the sub-domain. Details of the meteorological modeling and the VOC and NO_x emission inventory development for simulation of the full domain are available from the Texas Commission on Environmental Quality (TCEQ, 2004) and were described by Nam et al. (2006). Briefly, meteorological inputs were based on results from the NCAR/Penn State Mesoscale Meteorological Model version 5, MM5. Emission inventories, including emissions for mobile sources, area sources, biogenic sources, and point sources were prepared by the TCEQ. The flare emissions were then replaced with the stochastically generated emissions, leaving all other emissions unchanged. Both the sub-domain modeling and the full domain modeling in the region with industrial emissions were performed at a 1 km spatial resolution.

The full domain model was used to establish initial conditions and time varying boundary conditions for the sub-domain model. Calculations reported by Nam et al. (2006) indicate that the sub-domain model responds to temporal variability in industrial emissions in a manner that correlates ($r^2 > 0.96$) with the response of the full domain model. The sub-domain model was run for 25 August 2000. This date was selected because there was rapid ozone formation on this date and it shows one of the typical meteorological conditions that lead to high ozone concentrations. Details of the meteorological conditions on this date have been described by Nam et al. (2006).

3. Results and discussion

The results and discussion will be presented in two parts. The first part describes the effectiveness of control of allowable episodic component of flare emissions and the second part describes the effectiveness of control of the nearly constant component of flare emissions. All results reported in this analysis are in terms of 1-h averaged ozone concentrations; the impacts on 8-h ozone concentrations are left for future work.

3.1. Control of allowable episodic emissions

A total of 100 sets of stochastic emission inventories were generated with the models shown in Tables 1 and 3: 50 sets of inventories for simulation of emission variability without any emission control and 50 sets of inventories for simulation of emission variability with elimination of the allowable episodic emissions. Spatially detailed plots of ozone concentrations from individual cases discussed here can be found in Nam (2007). Since the stochastic inventory has both higher and lower VOC emissions across the HG area over the course of the day, ozone concentrations predicted using the stochastic inventory are both higher and lower than using the deterministic inventory without VOC emission variability, depending on time of day and location. In the

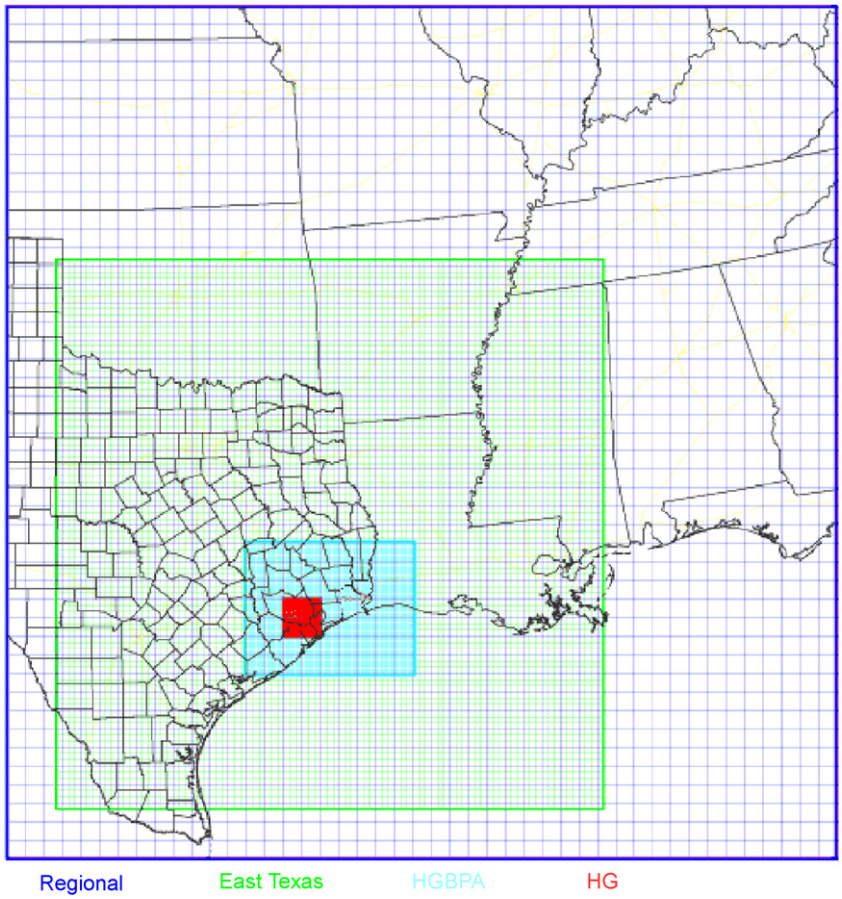

Fig. 3. Modeling domain used in the study. The Regional, East Texas, Houston–Galveston–Beaumont–Port Arthur (HGBPA), and Houston–Galveston (HG) nested domains had 36, 12, 4 and 1 km resolution, respectively.

inventory that led to the maximum increase in ozone concentration, ozone concentrations predicted using the stochastic inventory, without flare controls, are approximately 57 ppb higher than using the deterministic inventory without variable emissions. Ozone concentrations are also up to 7 ppb lower using this same stochastic inventory than using the deterministic inventory with constant industrial emissions.

Fig. 4 compares area-wide, daily maximum ozone concentrations, across the HG 1-km domain, using the stochastic inventories with no controls and the stochastic inventories with allowable episodic emissions control. For stochastic inventories without any flare emission control, the daily maximum ozone concentration ranges from 193.9 to 206.5 ppb, depending on the stochastic inventory used. The average of daily maximum ozone concentration using the 50 sets of stochastic inventories is 200.9 ppb (the area-wide maximum for the deterministic inventory was 200.6 ppb). For stochastic inventories with allowable episodic emissions eliminated, the daily maximum ozone concentration ranges from 193.3 to 204 ppb, depending on the stochastic inventory used. The average of the daily maximum ozone concentration with controls was 199.4 ppb, approximately 1.5 ppb decrease from the average of daily maxima without any emission control.

The average of the maximum difference in ozone concentrations (between the stochastic inventory with no controls and the deterministic inventories) over the 50 simulations with no controls is 24.8 ppb, Fig. 5a summarizes the maximum changes in ozone concentrations, both positive and negative, when all 100 sets of stochastic emission inventories were used for air quality simulations. Specifically, the quantity presented is the maximum difference in ozone concentration over the course of the day between using the stochastic inventory and the deterministic

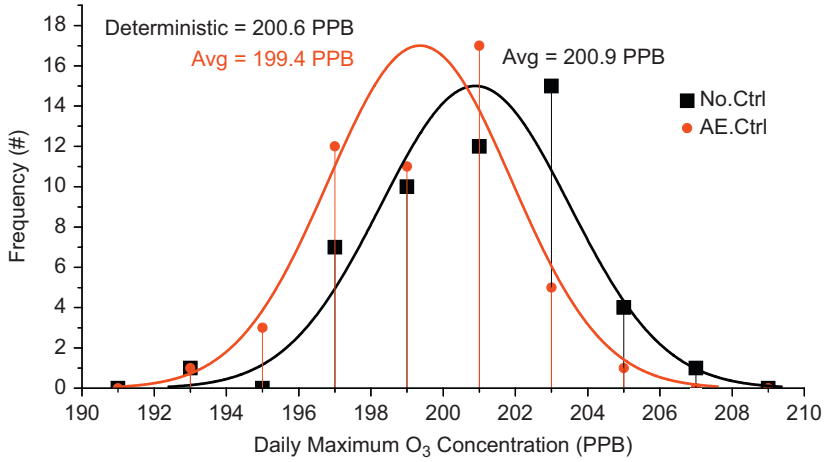

Fig. 4. Distributions of daily maximum ozone concentration across the HG 1-km domain for no control cases (black) and allowable episodic emission control cases (red).

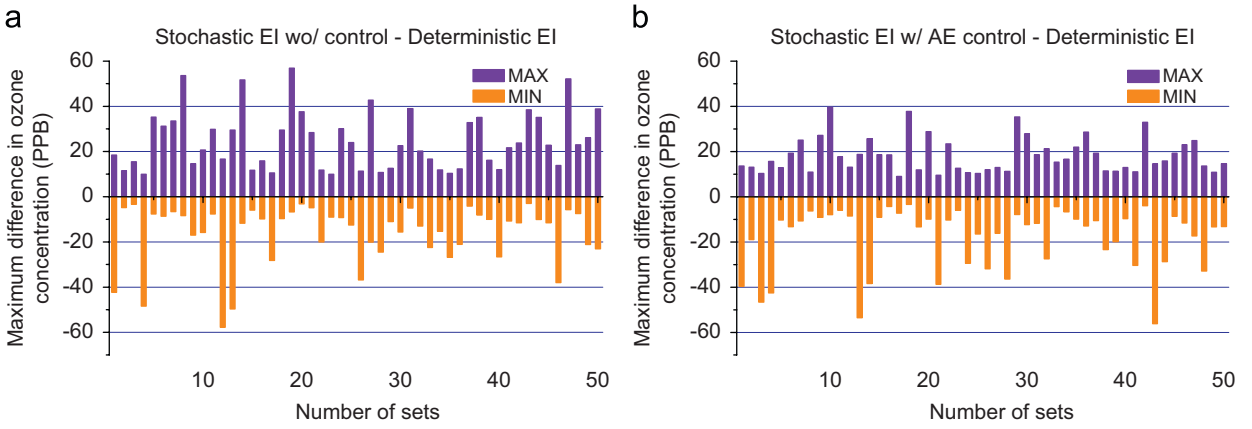

Fig. 5. Maximum difference in ozone concentration in 1-day simulations representing 25 August 2000. The difference is taken between the deterministic inventory with constant industrial emissions and the stochastic inventory for 50 instances of the stochastic inventory with allowable episodic emission without control (a) and with control (b).

inventory. In the simulation of ozone without any emission control, the maximum difference in ozone concentration is largest when the 19th stochastic inventory was used; the ozone concentrations are 24.5 and 81.4 ppb when the deterministic and the stochastic inventory were used, respectively, at conditions that lead to the maximum increase in ozone concentration. This result is analogous to the results shown by Webster et al. (2007), except that for this study the updated version of stochastic inventory generator was used, as described in the Methods section. Averages of the maximum difference between the stochastic and deterministic inventories reported by Webster et al. (2007) is 24.5 ppb, which is very close to the value of 24.8 ppb for the modified stochastic inventory generator.

Fig. 5b shows the same results for the cases where the allowable episodic flare emissions were eliminated. The magnitude of increase in ozone concentration was smaller and the magnitude of decrease was larger. The average of the maximum difference in ozone concentrations (between the stochastic inventory with allowable episodic emission controls and the deterministic inventories) is 18.2 ppb, over the 50 simulations. Probability distributions of the maximum difference in ozone concentration, both positive and negative, are shown in Fig. 6. The distribution of maximum increases in ozone concentration, shown in Fig. 6b, has a shorter tail to the right for the case when allowable episodic emissions are eliminated, as compared to the stochastic inventory results with no controls.

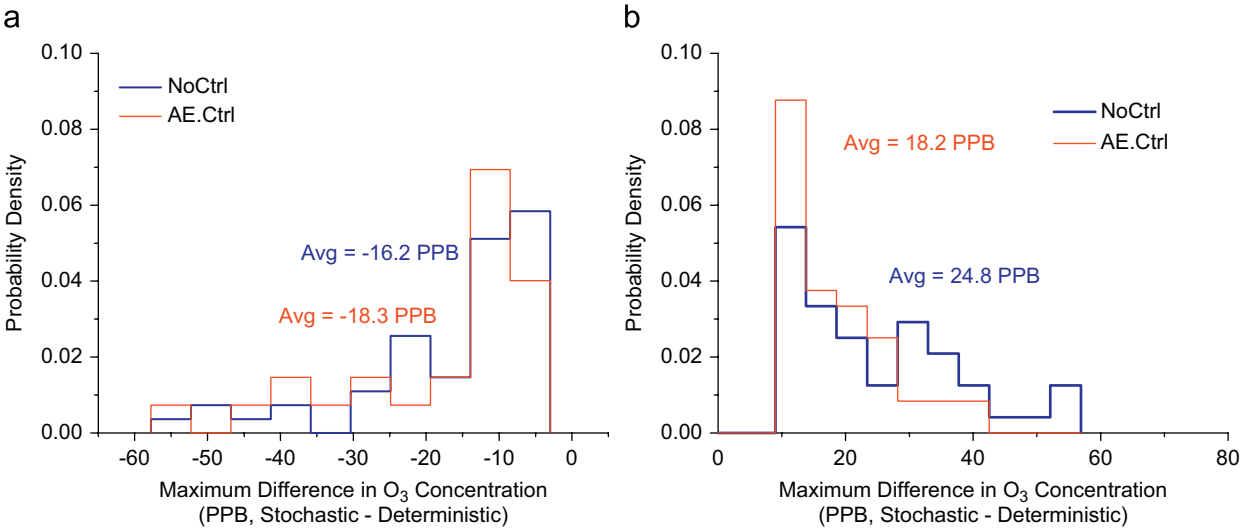

Fig. 6. Probability distribution of maximum changes in ozone concentration in simulations representing 25 August 2000 due to variable continuous emissions with allowable episodic emission control (red line) and without the control (blue line) in negative direction (a) and positive direction (b).

For comparison purposes, another control scheme was devised so that the same magnitude of reduction in total flare emissions occurred across the domain as when allowable episodic emissions are eliminated, but those reductions are applied to the deterministic inventory. This results in 2.1% and 4.3%, reductions in NO_x and VOC emissions, respectively. The maximum difference in ozone concentration was approximately 1.4 ppb. Daily maximum ozone concentration was decreased by just 0.1 ppb due to the emissions reductions in the deterministic inventory. This reduction in daily maximum ozone is smaller, by a factor of 11, than the average reduction in daily maximum ozone concentration (200.9 vs. 199.4, or 1.5 ppb) due to an equivalent mass reduction in allowable episodic emissions, as shown in Fig. 4.

3.2. Control of nearly constant emissions

The second control approach involves reduction in nearly constant emissions of NO_x and VOC emissions for all the flares in the HG domain. The stochastic inventory generator was modified to reflect this control scheme, as shown in Table 4, and a total of 50 sets of stochastic emission inventories were generated with the models. As described in the previous section, expected values of the nearly constant emissions were decreased by 50% by reducing means or shift values, depending on the distribution type (normal or lognormal).

Fig. 7 compares daily maximum ozone concentration in the HG domain for no control, for allowable episodic emission control, and for nearly constant emission control cases. Control of nearly constant emissions reduces the average peak ozone concentration by 10.5 ppb, versus a 1.5 ppb reduction for the control of allowable episodic emissions, however, the tons of emission reductions are different in the two cases. On average, total flare emissions across the domain were decreased, due to control of allowable episodic emissions, by 1.4 and 0.12 tons for VOC and NO_x, respectively, relative to no control cases. Reduction in daily maximum ozone concentration due to the control is 1.0 ppb per ton of VOC plus NO_x reduction (1.5 ppb 1.5 $tons^{-1}$). Control of nearly constant emissions reduced total flare emissions by 9.73 and 1.47 tons, for VOC and NO_x, respectively. Reduction in daily maximum ozone concentration is 0.9 ppb per ton of VOC plus NO_x reduction (10.5 ppb 11.2 $tons^{-1}$). Thus, the two strategies are equally effective, per ton, in reducing average peak ozone concentration. There is more mass of nearly constant emissions available for reductions, however, so these emissions provide a larger potential for change in average daily maximum ozone concentrations. As shown in Fig. 9, however, for eliminating the highest values of localized changes in ozone

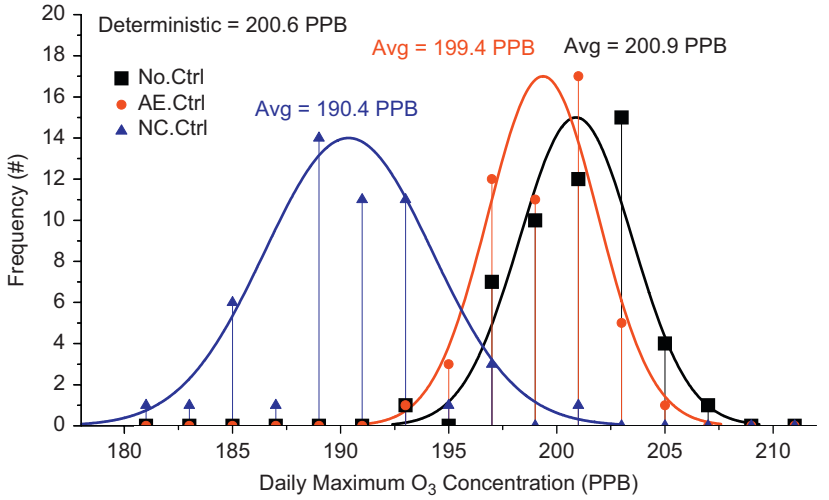

Fig. 7. Distributions of daily maximum ozone concentration across the HG 1-km domain for no control cases (black), allowable episodic emission control cases (red), and nearly constant emission control cases (blue).

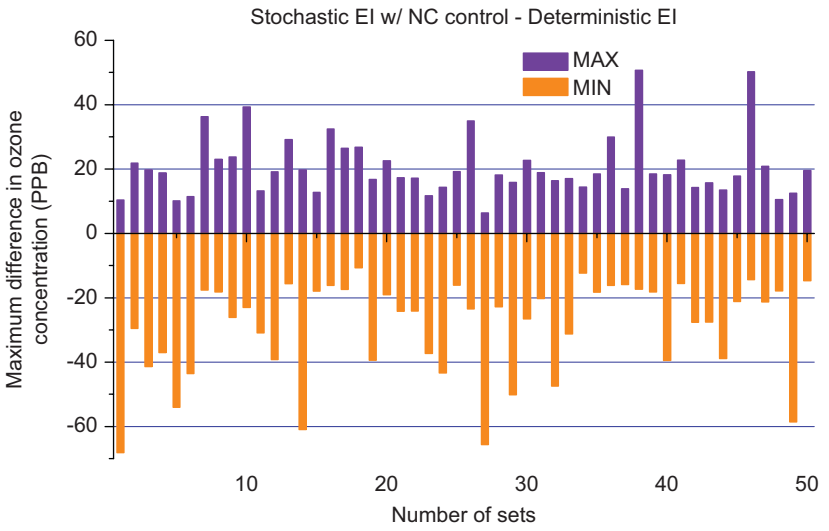

Fig. 8. Maximum difference in ozone concentration in 1-day simulations representing 25 August 2000. The difference is taken between the deterministic inventory with constant industrial emissions and the stochastic inventory for 50 instances of the stochastic inventory with a 50% reduction in nearly constant flare emissions. Maximum difference in ozone concentration was scaled to the results shown in Fig. 7.

concentrations, reducing allowable episodic emissions is a more effective strategy than reducing nearly constant emissions.

Fig. 8 summarizes the maximum changes in ozone concentrations, both positive and negative, when the 50 sets of stochastic emission inventories with a 50% reduction in nearly constant flare emissions were used for simulations. The maximum difference in ozone concentration is largest when the 38th stochastic inventory was used; the ozone concentrations are 47.4 and 98.1 ppb when the deterministic and the stochastic inventory were used, respectively, at conditions that lead to the maximum increase in ozone concentration. Fig. 9 compares the maximum difference in ozone concentration, both positive and negative, for eliminating allowable episodic emissions, for 50% reduction in nearly constant emissions, and for no control cases. Controlling the nearly constant emissions is not as effective in eliminating large maximum increases in ozone as controlling the allowable episodic emissions, however, reducing nearly

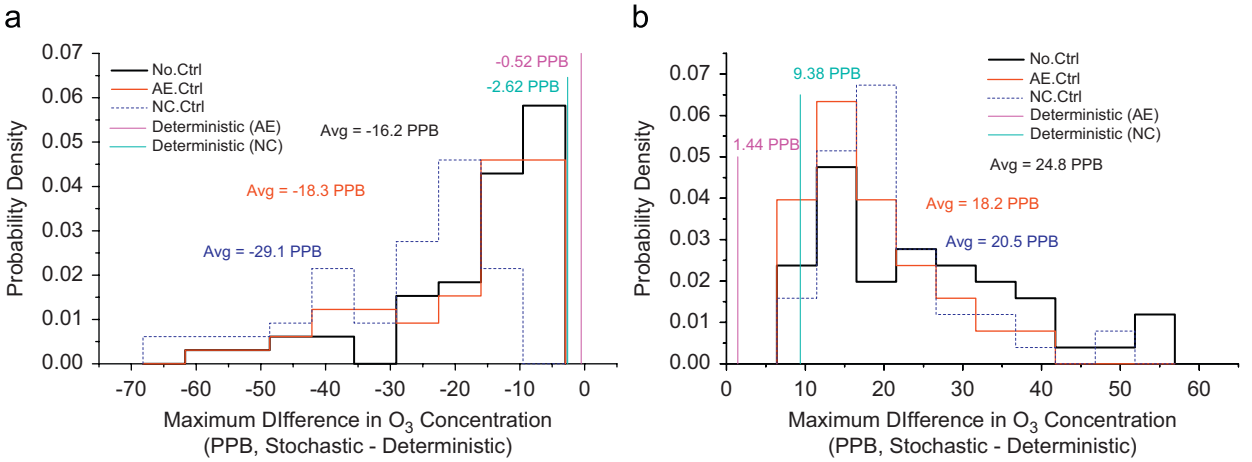

Fig. 9. Probability distributions of maximum changes in ozone concentration in simulations representing 25 August 2000 due to various emission controls in the stochastic inventory and due to the equivalent reductions applied to deterministic inventory in negative direction (a) and positive direction (b).

constant emissions generates larger maximum decreases in ozone concentrations.

For comparison purposes, the same magnitude of reduction in total flare emissions, due to nearly constant emission control, were applied to the deterministic inventory. The average daily maximum ozone concentration using the reduced deterministic inventory is 198.7 ppb, approximately 1.9 ppb lower than using the base case deterministic inventory. This decrease in daily maximum ozone concentration was more than a factor of 5 smaller than the average decrease in daily maximum ozone shown in Fig. 7.

4. Conclusions

This study evaluated two flare reduction scenarios as examples of alternative strategies for reducing ozone concentrations due to variable industrial emissions. The first control strategy involved reducing large magnitude, infrequent emissions (allowable episodic emissions) from flares and the second strategy involved reducing continuous, and relatively constant, emissions (nearly constant emissions) from flares.

In reducing changes in the daily maximum ozone concentrations over the 1-km domain, the two strategies are equally effective on a per-ton basis in reducing average peak ozone concentration. More mass of nearly constant emissions is available for reductions, however, so these emissions provide a larger potential for change in average daily maximum ozone concentrations. In contrast, for eliminating the highest values of localized changes in ozone concentrations, reducing allowable episodic emissions is a more effective strategy than reducing nearly constant emissions. For both control cases, maximum increases and decreases in ozone concentrations were significantly larger than those due to equivalent reductions in VOC and NO_x emissions applied to deterministic inventories.

The relative costs of different strategies are not addressed here; such an analysis is a separate study in its own right. However, if the costs of controlling the infrequently occurring higher emissions from flares (and other industrial point sources) is the same or less than that of reducing emissions all the time, this analysis suggests that targeting these highest emissions could be both cost-effective and achieve greater reductions in the worst high ozone events. Further work is needed, both to analyze the relative costs of different control strategies and to explore the impacts on 8-h ozone concentrations.

References

Bay Area Air Quality Management District (BAAQMD), 2005. Flare Monitoring at Petroleum Refineries, Accessed January 2007 at 〈http://www.baaqmd.gov/dst/regulations/rg1211.pdf〉.

Bay Area Air Quality Management District (BAAQMD), 2006. Flares at Petroleum Refineries, Accessed January 2007 at 〈http://www.baaqmd.gov/dst/regulations/rg1212.pdf〉.

Kleinman, L.I., Daum, P.H., Imre, D., Lee, Y.N., Nunnermacker, L.J., Springston, S.R., Weinstein-Lloyd, J., Rudolph, J., 2003. Correction to "Ozone production rate and hydrocarbon reactivity in 5 urban areas: a cause of high ozone

concentration in Houston". Geophysical Research Letters 30 (12), 1639.

Levy, R.E., Randel, L., Healy, M., Weaver, D., 2006. Reducing emissions from plant flares. In: Proceedings of the Air & Waste Management Association's Annual Conference, Paper ♯61.

Murphy, C.F., Allen, D.T., 2005. Hydrocarbon emissions from industrial release events in the Houston–Galveston area and their impact on ozone formation. Atmospheric Environment 39 (21), 3785–3798.

Nam, J., 2007. Variability in industrial hydrocarbon emissions and its impact on ozone formation in Houston. Ph.D. Thesis, University of Texas, Texas.

Nam, J., Kimura, Y., Vizuete, W., Murphy, C.F., Allen, D.T., 2006. Modeling the impacts of emission events on ozone formation in Houston, Texas. Atmospheric Environment 40 (28), 5329–5341.

Ryerson, T.B., Trainer, M., Angevine, W.M., Brock, C.A., Dissly, R.W., Fehsenfeld, F.C., Frost, G.J., Goldan, P.D., Holloway, J.S., Hubler, G., Jakoubek, R.O., Kuster, W.C., Neuman, J.A., Nicks, D.K., Parrish, D.D., Roberts, J.M., Sueper, D.T., Atlas, E.L., Donnelly, S.G., Flocke, F., Fried, A., Potter, W.T., Schauffler, S., Stroud, V., Weinheimer, A.J., Wert, B.P., Wiedinmyer, C., Alvarez, R.J., Banta, R.M., Darby, L.S., Senff, C.J., 2003. Effect of petrochemical industrial emissions of reactive alkenes and NO_x on tropospheric ozone formation in Houston, Texas. Journal of Geophysical Research 108 (D8), 4249.

Shell Oil Products US, 2006. Shell Martinez Refinery Flare Minimization Plan, submitted to Bay Area Air Quality Management District, September 2006.

Texas Commissions on Environmental Quality (TCEQ), 2004. Revisions to the State Implementation Plan for the Houston–Galveston–Brazoria nonattainment area. Accessed February 2007 at 〈http://www.tceq.state.tx.us/assets/public/implementation/air/sip/sipdocs/2004-05-HGB/execsumm.pdf〉.

Webster, M., Nam, J., Kimura, Y., Jeffries, H., Vizuete, W., Allen, D.T., 2007. The effect of variability in industrial emissions on ozone formation in Houston, Texas. Atmospheric Environment 41 (40), 9580–9593.